Semnan University

Progress in Engineering Thermodynamics and Kinetics Journal

Journal homepage: https://jpetk.semnan.ac.ir/

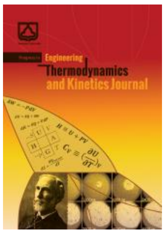

Research Article

Spectrophotometric and kinetic studies on electro-chemical decolorization of dyes in mixtures: combination of classical least squares and hard modelling approaches

S. Maryam Sajjadi *

Department of Chemical Engineering, Lamerd Higher Education Center, Shiraz University of Technology, Fars, Lamerd, Iran.

ARTICLE INFO

Article history:

Received: 202*-**-**
Revised: 202*-**-**
Accepted: 202*-**-**

Keywords:

Signal overlapping;
Multivariate analysis;
Electro-oxidation process;
Azo dyes;
Kinetic processes.

ABSTRACT

In this study, kinetic electro-oxidations of four dyes were simultaneously evaluated on a Ti/ZnO-multi-walled carbon nanotubes anode. The mixture of dyes includes acid red 33 (AR33), reactive orange 7 (RO7), acid yellow 3 (AY3) and malachite green (MG). The kinetic processes were monitored spectrophotometrically. Time-spectral data were analyzed in the time range of 0 to 80 min and wavelength range of 220-700 nm which suffers from signal overlapping of components. To obtain the kinetic degradation profiles of the components, the whole data set was resolved by the classical least squares method as a reliable method for analysis of data in which there are no selective responses for the analytes. Then, the kinetic rate constant of each dye decolorization together with its uncertainty was estimated by applying a hard modelling approach. The obtained rate constants were 0.0675 s^{-1}, 0.0262 s^{-1}, 0.0168 s^{-1} and 0.0158 s^{-1} for MG, AR33, AY3 and RO7, respectively, revealing that MG is the most degradable dye.

---

* **Corresponding author.**
E-mail address: sajjadi@sutech.ac.ir

Cite this article as:

Sajjadi, S.M. (2025). Spectrophotometric and kinetic studies on electro-chemical decolorization of dyes in mixtures: combination of classical least squares and hard modelling approaches. *Progress in Engineering Thermodynamics and Kinetics*, 1(2), pp.152-161.
https://doi.org/10.22075/jpetk.2024.30499.1014

1. Introduction

Water pollution as a crucial issue demands appropriate policy and techniques to prevent contamination of freshwater supplies and improve wastewater treatment. In recent years, the growth of population and industrial and agricultural expansion have led to an excessive rise in water consumption. The reports show there is wastewater discharge of about 1500 km^3 per year [1, 2]. The presence of synthetic compounds in effluent is really harmful to the environment and human health, even at trace levels, and it is required to eliminate these pollutants before wastewater discharge.

Among a variety of kinds of synthetic dye-stuff, azo-dyes have a significant portion in effluents while they have the least desirable consequences for surrounding ecosystems. These dyes are mainly resistant to aerobic degradation and they may produce carcinogenic aromatic amines in anaerobic conditions [3, 4].

Some conventional methods such as air stripping, extraction, ultrafiltration, and carbon adsorption have been employed for the removal of azo-dyes from wastewater. However, these techniques are non-destructive and they commonly transfer the pollutants from one phase to the other without decomposing them [5, 6]. In recent years, advanced oxidation processes (AOPs) have gained widespread application in degrading industrial wastewater due to their ability to decompose dyes in aqueous solutions [7-9]. Among AOPs, electrochemical advanced oxidation processes (EAOPs) are highly applicable for eliminating the dyes and oxidizing them during the removal processes. These methods possess some advantages such as cost-effectiveness, environmental friendliness, simplicity of operation, high removal efficiency, and prevention of secondary wastewater treatment [8,10].

The efficiency of EAOPs greatly depends on the anode material because electrochemical oxidation (EO) reactions occur between the electrode surface and solution, especially the production of °OH; therefore, the selection of the proper anode is a key factor in the remediation of dye-containing wastewater. In 2022, Mahmoudian et al. fabricated a titanium electrode coated with a nanocomposite of ZnO-multi-walled carbon nanotubes (ZnO-MWCNTs) by the electrophoretic deposition (EPD) method and applied it for the remediation of a water solution containing different dyes including Acid red 33 (AR33), Reactive orange 7 (RO7), Acid yellow 3 (AY3) and Malachite green (MG) [8]. They investigated the performance of the constructed Ti/nanoZnO-MWCNTs electrode in the EO processes of these dyes in a mixture, as a target for wastewater.

They monitored the EO reactions using a cost-effective and simple spectrophotometric technique where the analysis of the data was impossible using univariate techniques due to the signal overlapping of the dyes. To overcome this problem, they proposed a multivariate calibration technique to find the concentration of each dye at the final time of the decolorization process.

EAOPs are kinetic processes intrinsically, and the reaction rate constants of decolorization reactions permit a chemist/chemical engineer to design, operate, control, and optimize the reactors of the chemical industries. For instance, it could be checked if the process is in or out of control. A kinetic process can be monitored spectroscopically, and there are special multivariate resolution methods developed to estimate reaction rate constants and underlying spectra [11-15]. Although most wastewaters are composed of different contaminants, to the best of our knowledge, there is no report on the determination of simultaneous EO rate constants of several dyes with severely overlapped signals, and it is a neglected issue in EAOPs systems.

2. Experimental

2.1. Electrochemical oxidation of the dyes Procedure

The batch electrolytic cell reported in [8] was applied in this study to conduct electrochemical oxidation of the dyes. A mixture of the dyes was prepared in a 250 ml cylindrical glass reactor, in which the concentrations of dyes were 25, 25, 10 and 10 mg L^{-1} for AR33, RO7, AY3 and MG, respectively. The anode and cathode electrodes were a Ti/nanoZnO-MWCNT electrode and a stainless-steel plate (dimensions: 3×3 cm; thickness: 1 mm). The solution was stirred throughout the experiment to ensure efficient mass transfer. To monitor the decolorization process, 3 ml of the sample was withdrawn from the cell at a given time and its spectrum was obtained using a UV–Visible spectrophotometer with a 0.5 nm interval in the wavelength range of 200–800 nm. It was observed that the signals at wavelengths greater than 700 nm were not significant; moreover, there were no significant changes in signals at wavelengths less than 220 nm. Therefore, the data were selected in the wavelength range of 220-700 nm for further analysis. Indeed, a two-way data set was obtained at 966 wavelengths and 12 electro-oxidation times from 0 to 80 min where no significant changes were observed in the signals.

3. Theory

3.1. Classical Least Squares

The intentional objective in chemical systems is commonly the assessment of concentrations of individual components (*C*) or the recognition of unknown spectral profiles (*S*) in mixture solutions. The CLS model has the capability to calculate each *C* when *S* is known or vice versa. This strategy is based on the following matrix equation:

$$\boldsymbol{X} = \boldsymbol{C} \times \boldsymbol{S}^{\boldsymbol{T}} + \boldsymbol{R} \qquad (1)$$

Where *X* is the prime raw data matrix with the mixed experimental information. In this way, the columns in *C* and their corresponding rows in S^T consist of pure concentration and spectral profiles of the components involved in the data *X*, respectively, and *R* is the residual matrix. When the pure spectral components are known, matrix C can be obtained based on the least squares minimization of $\|R\|$, written as follows [16]:

$$\mathbf{C}=\mathbf{X}(\boldsymbol{S}^T)^+ \qquad (2)$$

Where the sizes of the relevant matrices are X (I×J), C (I×N), S (J×N), and E (I×J); and I, J, and N are the number of degradation times, wavelengths, and spectroscopically active components, respectively.

3.2. Hard-Modelling Technique

The hard-modelling method is an iterative process and calculates the best set of independent parameters in a defined model based on a least-squares algorithm. In this method, the goal is minimizing the sum of squares (SSQ), which is a function of a chemical model and its parameters [11, 12]:

$$\text{SSQ}= \sum_{i=1}^{i=m} \sum_{j=1}^{i=n} (R_{i,j}^2)=\text{f}\ (\mathbf{C}, \text{model, parameters}) \qquad (3)$$

The parameters are linear and non-linear, attributed to the elements of each column vector in matrix C and the kinetic constants involved in matrix C, respectively. It should be mentioned that the linear parameters can efficiently be eliminated during the iteration process. Indeed, the hard modelling strategy is a robust analysis technique because it fits a few number of parameters, i.e., the non-linear ones. In this work, the *lsqnonlin* Matlab command, based on the Newton-Gauss Levenberg Marquardt (NG/LM) algorithm, is used to conduct the fitting. During the optimization, the concentration profiles of species are calculated by first-order kinetic equations.

Indeed, many chemical processes are of a first-order nature or can be at least experimentally observed under pseudo-first-order conditions in which estimating the rate constants is not dependent on initial concentrations [14, 15].

4. Results and Discussion

The time-spectral data of electrochemical oxidation of a synthetic dyes mixture are depicted in Figure 1. To achieve the pure spectral profiles of the dyes, a standard solution of each dye (40 ppm) was prepared and its spectrum was recorded using a UV-Vis spectrophotometer at the same wavelength range as in the electro-oxidation processes' monitoring. It should be noted that these obtained spectra are the same as their corresponding pure profiles in shape but different in intensity.

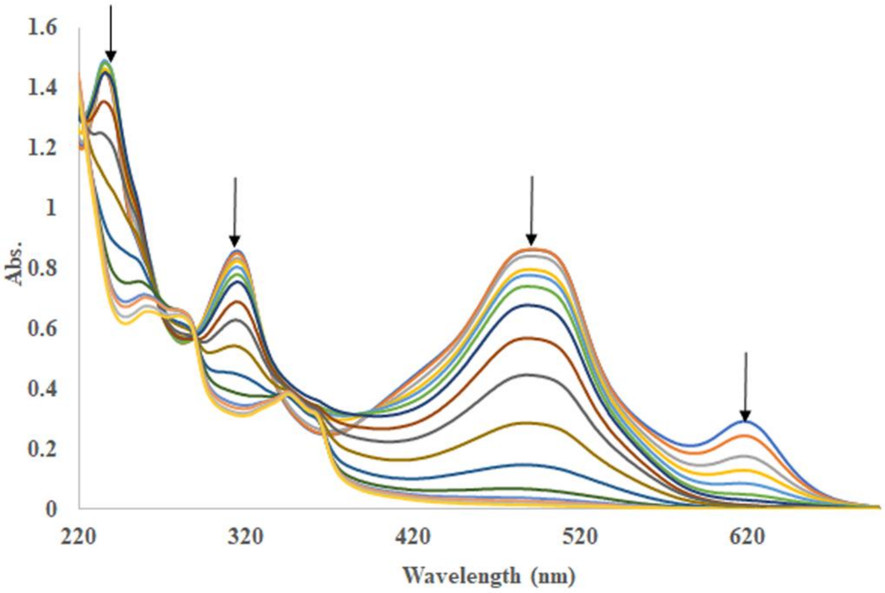

Fig 1. Time-spectral data of in synthetic mixtures of dyes containing AR33 (25 mgL^{-1}), RO7 (25 mgL^{-1}), AY3 (10 mgL^{-1}) and MG (10 mgL^{-1})

Given that, in a first-order reaction, the rate constant of the kinetic process can be estimated when the initial concentration of analyte is unknown, all the recorded spectra of standard solutions were normalized as illustrated in Fig. 2. Then the CLS model was applied to the data under these normalized pure spectral profiles (S in Eq. (2)) to obtain the kinetic profiles of the components; however, the profiles were not reliable, for example, there were not unimodal or some of their values were negative, as we know, a negative value for the concentration of a component is vague.

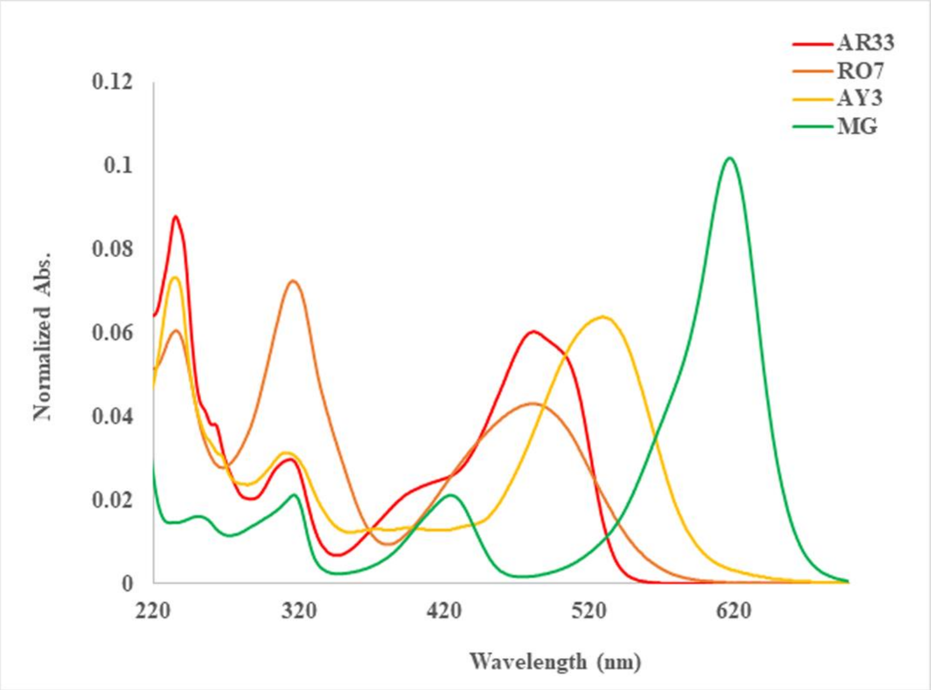

Fig 2. Normalized pure spectral profiles of the dyes

As seen in Fig. 1, the signals of the components are severely overlapped in the wavelength range of 220-400 nm and this part of the data possesses low information due to the lack of selectivity. Thus, we omitted this part from the data and pure spectral profiles, and then the CLS model was employed on the remaining data under the normalized pure spectral profiles. The obtained concentration profiles have been illustrated in Fig. 3. To evaluate the ability of CLS analysis, the standard deviation of residuals of data analysis (s_{cls}) was computed based on the following equation:

$$s_{cls} = \sqrt{\frac{\sum_{i=1}^{I}\sum_{j=1}^{J}\mathrm{R}_{ij}^{2}}{I\times J-(N\times J)}} \tag{4}$$

Where R_{ij} is the element of the residual matrix R; and I, J and N are the same as in Equation (2).

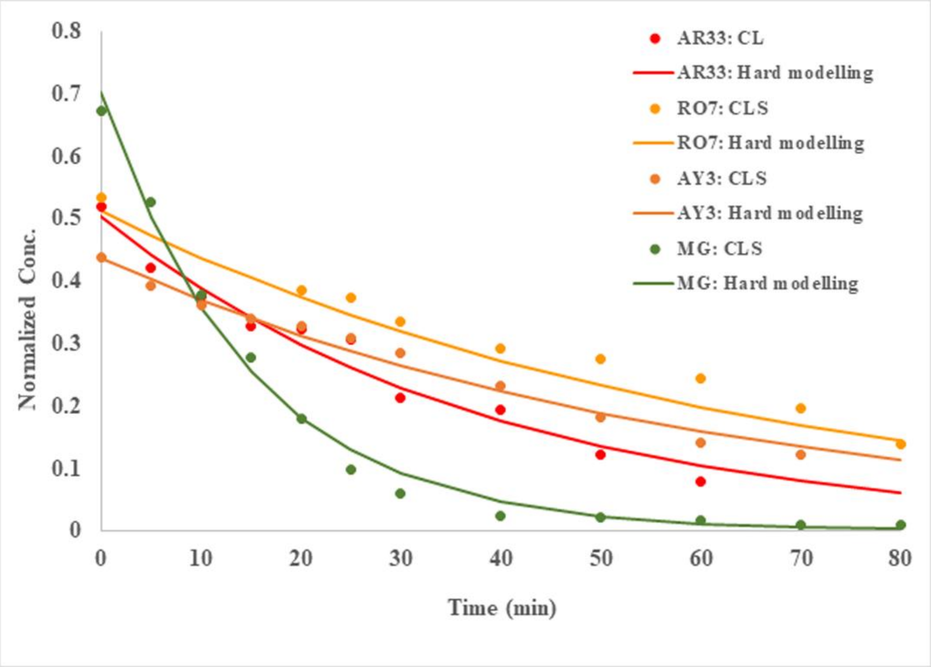

Fig3. Normalized concentration profiles of the dyes obtained by CLS method (Paint) and hard modelling approach (Solid line)

The calculated s_{cls} was 0.0173, which confirms the unmodelled part of the data is attributed to noise. To compute the rate constant of each dye decolorization (k), each kinetic profile was analyzed by the hard modelling approach based on the postulated first-order reaction $A \xrightarrow{k} B$ as follows:

$$A_t = exp(-kt) \tag{5}$$

Where the initial substrate is one, A_t is the concentration of the dye involved in a first-order reaction at electro-oxidation time t and k is the rate constant of the decolorization. Fig. 3 overlays the obtained normalized concentration profiles by the CLS method and their corresponding fitted profiles by the hard modelling approach. This figure reveals that the obtained normalized concentration profiles by the CLS method match well with those of the hard modelling approach. The estimated k values together with their corresponding standard deviations have been reported in Table 1. This table compares the rate constants of the degradation processes of the dyes and shows that MG is the most degradable component in this system as its rate constant is significantly high. It seems the structure of the dye molecule could be responsible for the degradation mechanism.

Table 1. The estimated decolorization rate constants of the dyes by hard modeling method

Dyes	k (min^{-1})
AR33	0.0262 (±0.002)
RO7	0.0158 (±4.95×10^{-4})
AY3	0.0168 (±8.94×10^{-4})
MG	0.0675 (±0.0034)

5. Conclusion

The main focus of this work is the kinetic study of the electrochemical oxidation degradation of a synthetic dyes mixture composed of AR33, RO7, AY3 and MG on a Ti/nanoZnO-MWCNTs electrode at the optimal operational parameters including pH, current, and electrolyte concentration with values, respectively. These simultaneous kinetic processes were monitored spectrophotometrically at a wavelength range of 400-700 nm where the signals of the components are highly overlapped, as it was not possible to obtain the kinetic profiles of the analytes. Here, the classical least square method was proposed to overcome this problem. Indeed, the multivariate analysis technique allows one to obtain the pure kinetic profiles of the degraded dyes, all of which are the same as the real pure profiles in shape but different in intensity.

To estimate the kinetic rate constant (k) of the degradation processes, the concentration profile of each component was fitted by the hard modelling approach based on the NG/LM algorithm, which computes both the k value and its standard deviation. The k*s* values were 0.0675 s^{-1}, 0.0262 s^{-1}, 0.0168 s^{-1} and 0.0158 s^{-1} for MG, AR33, AY3 and RO7, respectively, revealing that MG is the most degradable dye.

Acknowledgments

I deem it necessary to thank Dr. Farideh Nabizadeh-Chianeh and Miss Fatemeh Mahmoudian from Semnan University, whom I was their coworkers in the previous published work (cited reference No. 8), for providing me their electrochemical laboratory system studied in this work.

Funding Statement

This research did not receive any specific grant from funding agencies in the public, commercial, or not-for-profit sectors.

Conflicts of Interest

The author declares that there is no conflict of interest regarding the publication of this article.

References

[1] J. van der Geer, J.A.J. Hanraads, R.A. Lupton, The art of writing a scientific article, J. Sci. Commun. 163 (2010) 51–59.

[2] R. Kumar, et al., A review on emerging water contaminants and the application of sustainable removal technologies." Case Stud. Chem. Environ. Eng. 6 (2022) 100219-100232.

[3] M. Gu, Q. Yin, Z. Wang, K. He, G. Wu. Color and nitrogen removal from synthetic dye wastewater in an integrated mesophilic hydrolysis/acidification and multiple anoxic/aerobic process. Chemosphere. 212 (2018) 881-889.

[4] M. Jayapal, et al. Sequential anaerobic-aerobic treatment using plant microbe integrated system for degradation of azo dyes and their aromatic amines by-products. J. Hazard Mater 354 (2018) 231-243.

[5] M. R. Gadekar, M.M. Ahammed. Modelling dye removal by adsorption onto water treatment residuals using combined response surface methodology-artificial neural network approach. J Environ Manage. 231 (2019) 241-248.

[6] V. M. Esquerdo, et al., Kinetics and mass transfer aspects about the adsorption of tartrazine by a porous chitosan sponge. React. Kinet. Mech. Cat. 116 (2015) 105–117.

[7] M. Rashidi, S. M. Sajjadi, H. Z. Mousavi. Kinetic analysis of azo dye decolorization during their acid–base equilibria: photocatalytic degradation of tartrazine and sunset yellow. React. Kinet. Mech. Cat. 128 (2019) 555-570.

[8] F. Mahmoudian, F. Nabizadeh Chianeh, S. M. Sajjadi, Simultaneous electrochemical decolorization of Acid Red 33, Reactive Orange 7, Acid Yellow 3 and Malachite Green dyes by electrophoretically prepared Ti/nanoZnO-MWCNTs anode: experimental design. J. Electroanal. Chem. 884 (2021) 115066.

[9] T. P. Shende, Sonochemical synthesis of Graphene-Ce-TiO2 and Graphene-Fe-TiO2 ternary hybrid photocatalyst nanocomposite and its application in degradation of crystal violet dye. Ultrason. Sonochem. 41 (2018): 582-589.

[10] R. Berenguer, J.M. Sieben, C. Quijada, E. Morallón, Electrocatalytic degradation of phenol on Pt- and Ru-doped Ti/SnO2 Sb anodes in an alkaline medium. Appl. Catal. B: Environ 199 (2016) 394-404.

[11] M. Maeder, D. Z., Andreas, Nonlinear least-squares fitting of multivariate absorption data. Anal. Chem. 62 (1990)2 220-2224.13.

[12] K. J. Molloy, M Maeder, M. M. Schumacher. Hard modelling of spectroscopic measurements. Applications in non-ideal industrial reaction systems. Chemometrics Intell. Lab. Syst. (1999) 221-230.

[13] F. Chitgaran, S. M. Sajjadi, F. Nabizadeh Chianeh, J. Feizy, Spectrophotometric Study of Photo-electro-catalytic Degradation of 4-Nitrophenol on TiO2-MWCNT/Ti Electrode Using Multivariate Cure Resolution-Alternating Least Squares Method. Applied Chemistry Today 18 (2023) 235-250.

[14] S. M. Sajjadi, Z. Asadollah-pour, S. H. Sajjadi, S. N. Nabavi, Investigating photocatalytic degradation of o-nitrophenol and p-nitrophenol over efficient CoO-Fe 2 O 3@ SiO 2@ TiO 2 nanocomposite: rank annihilation factor analysis approach. *Chem. Pap. 76* (2022) 427-438.

[15] S.M. Sajjadi, et al., A thorough investigation of photo-catalytic degradation of ortho and para-nitro phenols in binary mixtures: new insights into evaluating degradation progress using chemometrics approaches." *New J. Chem.* 45 (2021) 12974-12985.

[16] N. B. Gallagher, Detection, classification and quantification in hyperspectral images using classical least squares models. *Techniques and applications of hyperspectral image analysis* 2007, pp. 181-201.